RSC Advances

ROYAL SOCIETY OF CHEMISTRY

www.rsc.org/advances

RSC Advances

Cite this: DOI: 10.1039/c0xx00000x

www.rsc.org/XXXXXX

PAPER

Synthesis and characterization of UV upconversion material Y_2SiO_5:Pr^{3+}, Li^+/TiO_2 with enhanced the photocatalytic properties under a xenon lamp

Jianhong Wu, Yanmin Yang*, Zhiren Wei, Boning Han, Jun Wei

Received (in XXX, XXX) Xth XXXXXXXXX 200X, Accepted Xth XXXXXXXXX 200X
DOI: 10.1039/b000000x

The upconversion luminescence agents Y_2SiO_5: Pr^{3+}, Li^+, that can be effectively excited by the blue light from a xenon lamp 150W with grating as its light splitter, are fabricated by a hydrothermal method with mesoporous molecular sieves of MCM-48 as the suitable silica source. The obtained emission spectra of Y_2SiO_5: Pr^{3+}, Li^+ and Y_2SiO_5: Pr^{3+}, Li^+/TiO_2 excited by a xenon lamp indicate that the UV upconversion luminescence of Pr^{3+} can be effectively transferred to TiO_2. The photocatalytic performances of Y_2SiO_5: Pr^{3+}, Li^+/TiO_2 are evaluated by the degradation of methylene blue upon xenon lamp irradiation. The degradation rate of the methylene blue with Y_2SiO_5: Pr^{3+}, Li^+/TiO_2 is 14 times as high as that with only TiO_2.

1. Introduction

With the growth of worldwide industry, severe environmental contaminations have become a major concern of our society. Photocatalysis, as an environmentally friendly technique in utilizing clean, safe, and renewable solar energy to eliminate toxic organic substances in air and water, has attracted considerable attention.[1-5] TiO_2 is known as the most widely investigated photocatalyst due to its high oxidative efficiency, high chemical stability, non-toxicity and low-cost.[6-8] Presently, the photocatalytic degradation activity of TiO_2 is still low, mainly due to the poor solar energy utilization. As is well known, TiO_2 with a bandgap of 3.2eV can be only excited by photons with light wavelengths shorter than about 400 nm in the UV wavelength range, which accounted for about 4% of the solar radiation energy.[9] It is of interest to find a TiO_2-based photocatalyst which is sensitive to visible light (~48%) and near infrared-light (~44%) in order to make more efficient use of solar energy in practical applications. Numerous methods had been adopted, such as surface modification,[10, 11] metal or nonmetal elements doping,[12-15] and the combination with a visible light excited semiconductor (narrow band-gap semiconductor such as CdS, CdSe, CdSSe) and so on.[16-20]

Recently, the upconversion luminescence agent that could transform the visible-light and near infrared-light into the ultraviolet light to satisfy the genuine requirement of TiO_2 catalysts became the investigated subject.[21-23] It is generally known that the upconversion emission power p is proportional to $\phi^n (n \geq 2)$ (ϕ for the excitation density). So the upconversion emission power p would quickly decreased in magnitude as the excitation density ϕ decreased. When the excitation density ϕ decreased to a certain threshold value, the upconversion emission power p is close to zero. This threshold value is very high for general materials, about $1mW/\mathrm{cm}^2$.[24, 25] So almost all of the upconversion luminescence emissions can only be achieved under the laser excitation. Although laser can be used as the driving source for photocatalysis, it may not be practical in view of its small excitation area.[26-29] In this scenario, only the point light source such as fluorescent lamp or xenon lamp, and also the area light source such as sunlight irradiation are meaningful for application. But those sources are polychromatic light and the excitation density of the effective light is relatively lower compared with laser, it is difficult to achieve upconversion luminescence. Now let's comprare the excitation density of fluorescent lamp and fiber laser. The illumination area (light spot) is fixed at $1\mathrm{cm}^2$, the power of fiber laser and fluorescent lamp is 1W and the distance from light sources to samples is fixed at 10 cm. So, the energy density of excitation light of fiber laser is $1/\pi(10\times0.22)^2 = 65.7\ mW/cm^2$ (0.22 is the divergence angle provided by manufacturers) and the energy density of excitation light of fluorescent lamp is $1/4\pi(10)^2/20 = 0.04\ mW/cm^2$ (20 is the effective wavelength width of the visible-light). The excitation density of the fiber laser is 1642 times as high as the fluorescent lamp.

To make upconversion materials used for photocatalysis, it is necessary to reduce the threshold of the energy density of excitation light. Simultaneously, the excitation range of the activation center should be as wide as possible so as to improve the utilization rate of the excitation light. Rare earth ions have been commonly considered as the luminescence center in upconversion process, for example Er^{3+}, Ho^{3+} and Tm^{3+}. Er^{3+} ions can produce efficient ultraviolet (UV) emissions under the excitation of green or blue lasers.[30, 31] Recently, some reports demonstrated that TiO_2 photocatalysis behavior was extremely

enhanced by doping Er^{3+} ions under visible light irradiation.[32-39] However, it still raises the question of whether UV upconversion emissions result in the enhanced photoactivities because no emission spectra have been given under a xenon lamp excitation. If upconversion emission cannot be achieved under 150W xenon lamp excitation (the minimum power excitation source for spectrometers), it is hardly realistic for upconversion materials to be used for photocatalysis. Our previous works have reported UV upconversion emission of Er^{3+} upon 1W 532nm LED and 300mW 460nm LED irradiation.[40] So, it is possible for Er^{3+} doped upconversion material to be used in many fields, such as biology application and photocatalysis. However, the narrow absorption range in visible light region prevents its practical use in the fields of biology and photocatalysis. Y_2SiO_5: Pr^{3+}, Li^+ can emit a wide UV radiation of 260-360nm under blue, green even red light excitation.[41] Ezra L *et al.* have systemically investigated this material and successfully used it in microbial inactivation with two "cool white" 13W compact fluorescent bulbs radiation.[42] All of those provide a possible for Y_2SiO_5: Pr^{3+}, Li^+ to be used for photocatalysis.

In this work, in order to make TiO_2 fully absorbed, Y_2SiO_5: Pr^{3+}, Li^+ was synthesized using mesoporous silica (MCM-48) as the silica source material. The obtained data showed that Y_2SiO_5: Pr^{3+}, Li^+ can be effectively excited by 496nm light obtained by a 150W xenon lamp spectrometer (Hitachi F-4600). Afterwards, Y_2SiO_5: Pr^{3+}, Li^+/TiO_2 composites were prepared through the ultrasonic dispersion and liquid boiling method. The photocatalytic property of the sample was examined in detail by decomposing the methylene blue. The results demonstrated that the visible-light photocatalytic activity of TiO_2 could be significantly enhanced in the presence ofY_2SiO_5: Pr^{3+}, Li^+.

2. Experimental section

2.1 Synthesis of MCM-48 powders

The homogeneous precipitation method was used for the preparation of mesoporous silica MCM-48. At first, cetyltrimethylammonium bromide ($C_{16}H_{33}(CH_3)_3NBr$, 0.0143 mol), ammonia solution ($NH_3 \cdot H_2O$, 24 ml), ethanol (CH_3CH_2OH, 100 ml) as well as deionized water (H_2O, 240 ml) were mixed by stirring magnetically until the homogenous solution was obtained. Then, tetraethylorthosilicate (TEOS, 7.8 ml) was added dropwise into the above mixed solution and further stirred until the transparent sol was successfully formed. After filtration and lavation, the separated deposit was calcined at 550°C for 5 h, and then cooled down to room temperature naturally.

2.2 Synthesis of Y_2SiO_5: Pr^{3+}, Li^+ microcrystals

The various concentrations of Y_2SiO_5: Pr^{3+}, Li^+ microcrystals were synthesized via a hydrothermal method. Briefly, 0.03592 mol $Y(NO_3)_3 \cdot 6H_2O$, 0.00048 mol $Pr(NO_3)_3 \cdot 6H_2O$, 0.0018 mol Li_2CO_3 and 0.02 mol MCM-48 were dissolved into deionized water by the ultrasonic dispersion with 100W output power ultrasound. Then, 0.12 mol NaOH solution which should control the mole ratio of $n(OH^-):n(Y^{3+}+Pr^{3+}+Li^+)$ for 3:1 was added dropwise into the above suspension. After thorough stirring, the mixture was transferred into a 100 mL teflon lined stainless steel autoclave. The autoclave was sealed and maintained in an oven at 110°C for 20 h, and then cooled down slowly to room temperature. The product was centrifuged and washed by deionized water for several times. After drying in air at 60°C for 20 h, the particles were heated in a muffle furnace at 700°C - 1300°C for 4 h. At last, the desired white Y_2SiO_5: Pr^{3+}, Li^+ particles were obtained.

2.3 Preparation of Y_2SiO_5: Pr^{3+}, Li^+/TiO_2 composites

Y_2SiO_5: Pr^{3+}, Li^+/TiO_2 catalysts were prepared through the ultrasonic dispersion and liquid boiling methods in terms of the literature.[43] In a typical procedure, Y_2SiO_5: Pr^{3+}, Li^+ and TiO_2 powders (mole ratio for 5: 2) were added into a 200 mL beaker filled with 30 mL deionized water, adequately dispersed by ultrasound for 30 min. The suspended liquid was heated up to the boiling point and kept for 30 min. After filtration and lavation, the separated deposit was put into a crucible and heated in a muffle furnace. The temperature was controlled at 550°C for 90 min.

2.4 The evaluation of the photocatalytic performance

The photocatalytic performances of the obtained products were evaluated by the degradation of methylene blue (MB) in aqueous solution. In the experiment, 1.15 g of Y_2SiO_5:Pr^{3+}, Li^+/TiO_2 composite was dispersed into a teflon lined stainless steel reactor containing 80mL 10mg L^{-1} MB aqueous solution. Prior to irradiation, the reactor was kept in dark for 12 h for establishing an adsorption–desorption equilibrium of MB on the surface of photocatalysts. Then the suspensions were irradiated using a 500 W xenon lamp. A cut off filter (λ>400 nm) was fitted to the aforementioned light source to get the applicable light irradiation. After each irradiation, 6.0 mL of the MB aqueous solution was taken out for the absorbance measurements. The dye concentration was calibrated using the absorption peak at 664 nm of MB.

2.5 Characterizations

Phase identification was performed at ambient temperature by X-ray diffraction (XRD, Bruker Optics, Ettlingen, Germany) with Cu Kα radiation (40kV, 40mA). The emission (PL) spectra were measured by a spectrophotometer (Hitachi F-4600) equipped with a 150 W Xenon lamp source and double excitation monochromators. The morphology was characterized by SEM (JSM-7500FJEOL, Japan) with the operating voltage of 30.0 kV. Energy dispersive spectroscopy (EDS) was obtained on a JSM-7500F microscope coupled with an EDS spectrometer. The absorption spectra were recorded with a UV–NIR spectrophotometer (Hitachi U-4100). Fourier transformation infrared spectroscopy (FTIR, Tensor 27, Bruker, Germany) was employed to check the crystal and groups of samples. Similar photocatalysis experiments were carried out under the 500 W xenon lamp (CEL-LAX500) of sunlight to check the photocatalytic activity of the Y_2SiO_5: Pr^{3+}, Li^+/TiO_2 catalysts.

3. Results and Discussion

3.1 Structural and morphological characterizations

3.1.1 XRD, SEM and FTIR of MCM-48 powder

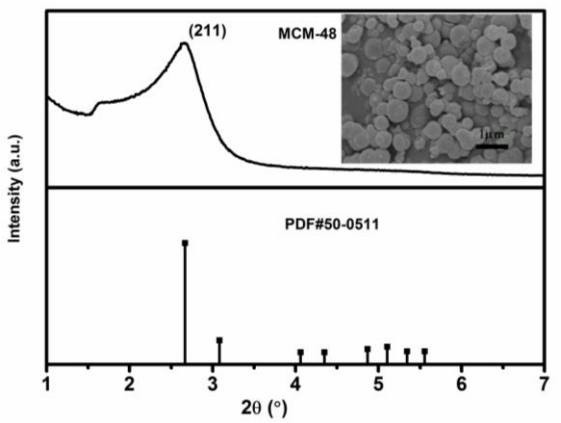

Fig.1 XRD pattern and SEM image of the as-prepared MCM-48 powder and the XRD pattern of the standard data of MCM-48 powder.

Fig.1 showed the XRD pattern and SEM image of the as-prepared sample. The XRD of the as-prepared sample reflected the intense diffraction peak of (211) plane approximately appeared at 2θ=2.6° that matched with the standard reference (PDF#50-0511), indicating the formation of MCM-48 mesoporous silica. According to Bragg equation ($2d\sin\theta = n\lambda$, λ = 0.154 *nm*, n = 1), the mesoporous channels calculated value of diameter d was 3.31 nm. The scanning electron image indicated that the average particle size of the as-prepared sample was about 400 nm.

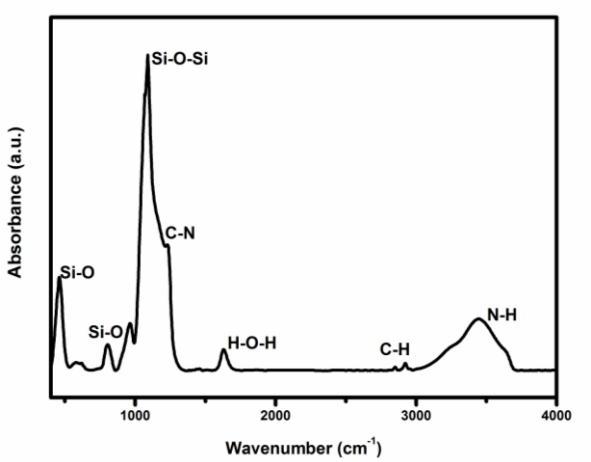

Fig.2 FTIR spectra of the MCM-48 powder.

Fourier transformation infrared spectroscopy (FTIR) was carried out to investigate the composition of the sample, as shown in Fig.2. The absorption band at 462.9, 811.9, 960.5 cm^{-1} could be attributed to the bending vibration, the stretching vibration as well as the asymmetric vibration of Si-O bond, respectively. Similarly, the Si-O-Si bond appeared at 1091 cm^{-1}. The absorption bands at 1260–1620 cm^{-1} were attributed to the bending vibration of O-H bond of H_2O, which was adsorbed on the internal holes from the surface of the mesoporous silica (MCM-48) in some ways. The other absorption bands, such as 1468, 1491, 2855, 2924 cm^{-1} and 3458 cm^{-1} were mainly derived from the vibration absorption of the quaternary ammonium surfactant (CTAB). It was shown that some organic residues still existed in the material.

3.1.2The crystal structure, surface profile, chemical character of Y_2SiO_5: Pr^{3+}, Li^+ microcrystal

The phase is related to the calcining temperature, the amount and type of dopants.[44] In this paper, we investigated the effect of sintering temperature and Li^+ doping concentration on the material structure. Table 1 showed the effects of sintering temperature as well as Li^+ concentration on the phase of Y_2SiO_5. The corresponding XRD pattern of Y_2SiO_5: Pr^{3+} was shown in Figure S1 and S2, Supporting Information.

Table 1 (a) the changing phase of Y_2SiO_5:Pr^{3+} doped with 0% and 9% Li^+, respectively, calcined at different temperatures from 700°C to 1300°C. (b) effect of various concentrations of Li^+ co-doped on the crystal structure of Y_2SiO_5:Pr^{3+} annealed at 1100°C.

(a)

Temperature °C	Phase(0% Li^+ co-doped)	Phase(9%Li^+co-doped)
700	Un-crystallization	Un-crystallization
800	Un-crystallization	Un-crystallization
850	Un-crystallization	α phase
900	α phase	α phase
950	α phase	α phase
1000	α phase	β phase
1100	α phase	β phase
1200	β phase	β phase
1300	β phase	β phase

(b)

Li^+ concentration%	0	5	7	8	9	10	11	15
phase 1100°C	α	α	β	β	β	β	β	β

From the obtaind data, it can be concluded that the calcinations temperature at 1100°C with the concentration of Li^+ above 7% allowed obtaining more suitable β phase structure.

3.1.3 The combination of Y_2SiO_5: Pr^{3+}, Li^+/TiO_2

Fig.3 (a) and (b) showed the morphologies of the as-prepared Y_2SiO_5: Pr^{3+}, Li^+ microcrystals and Y_2SiO_5: Pr^{3+}, Li^+/TiO_2 composites. The obvious agglomerates phenomenon could be observed in Fig.3 (b), which was resulted from the post-processing. The EDS spectra of synthesized Y_2SiO_5: Pr^{3+}, Li^+ and Y_2SiO_5: Pr^{3+}, Li^+/TiO_2 were shown in Fig.3 (c) and (d). Fig.3 (c) showed Pr particles percent content was 1.2%, which was approximate with the theoretical atomic ratio. Fig.3 (d) showed the ratio of Ti element was also similar with the precursor. All the data indicated that theTiO_2 nanocrystallites were well-mixed with Y_2SiO_5: Pr^{3+}, Li^+.

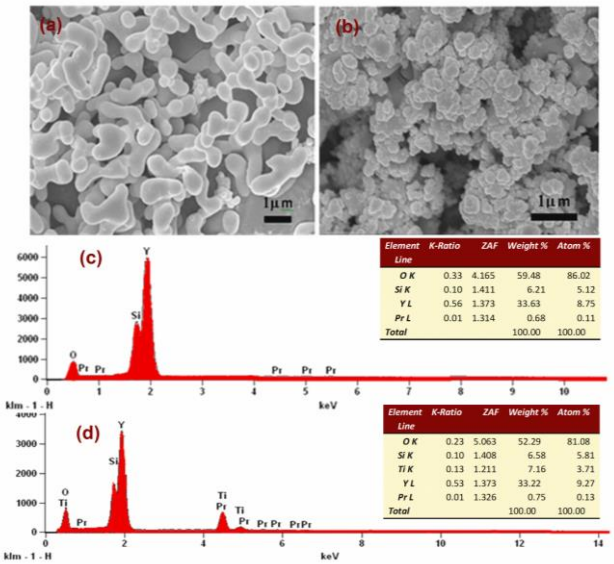

Fig.3 SEM images of Y_2SiO_5: Pr^{3+}, Li^+ microcrystals (a) and Y_2SiO_5: Pr^{3+}, Li^+/TiO_2 composites. (b) The corresponding EDS pattern (c) and (d).

3.2 Optical properties

3.2.1 The optical properties of Y_2SiO_5: Pr^{3+}, Li^+

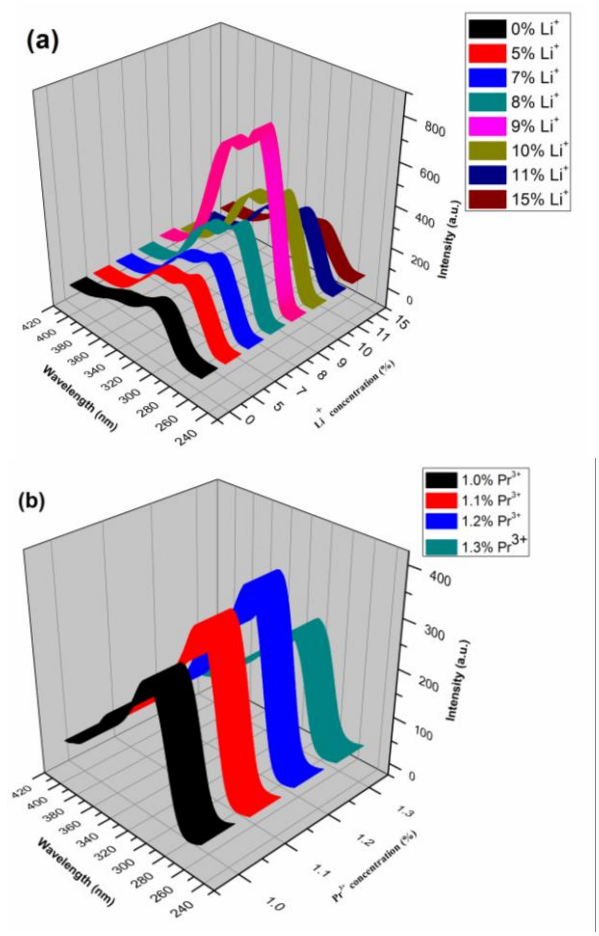

Fig.4 Upconversion emission spectra of Y_2SiO_5: x% Pr^{3+}, y% Li^+ excited by a xenon lamp 150 W with grating as its light splitter, calcined at 1100°C (a) Co-doped with different Li^+ concentration (x=1.2; y=0, 5, 7, 8, 9, 10, 11, 15); (b) Co-doped with different Pr^{3+} concentration (x=0.9, 1.0, 1.1, 1.2, 1.3; y= 9).

Upconversion emission spectra of Y_2SiO_5: Pr^{3+}, Li^+ with different dopant concentration were obtained by a xenon lamp 150W with grating as its light splitter, as shown in Fig.4. Upon the 496 nm excitation, the emission spectra in a broad range from 260 nm to 400 nm were obtained. With Li^+ concentration increasing, the upconversion emission intensity increased firstly and then remarkably decreased as shown in Fig 4 (a). The similar result can be obtained by doping Pr^{3+} ions. So, the strongest upconversion emission came from Y_2SiO_5: 1.2% Pr^{3+}, 9% Li^+ calcined at 1100°C.

3.2.2 The optical properties of Y_2SiO_5: Pr^{3+}, Li^+/TiO_2

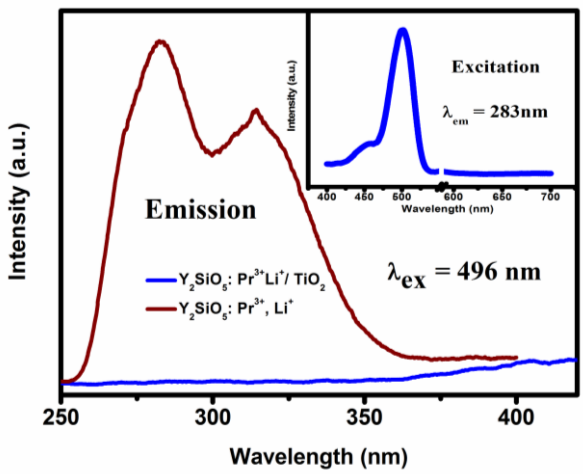

Fig.5 Upconversion emission spectra of Y_2SiO_5: Pr^{3+}, Li^+ phosphor powders and Y_2SiO_5: Pr^{3+}, Li^+/TiO_2 composites under 496 nm excitation by a xenon lamp 150W with grating as its light splitter, with the inset of excitation spectra (λ_{em} =283 nm) of Y_2SiO_5: Pr^{3+}, Li^+ in visible-light region.

Fig.5 showed the emission spectra of Y_2SiO_5: Pr^{3+}, Li^+ and Y_2SiO_5: Pr^{3+}, Li^+/TiO_2 composites under 496 nm excitation by a xenon lamp 150W with grating as its light splitter. The emission spectrum of Y_2SiO_5: Pr^{3+}, Li^+ microcrystals contained two emission peaks located at 288 nm (4.306eV) and 320 nm (3.875eV), respectively. It's worth noting that the emission spectrum of Y_2SiO_5: Pr^{3+}, Li^+ microcrystals disappeared while TiO_2 was adsorbed on their surface. It indicated that UV upconversion emission of Y_2SiO_5: Pr^{3+}, Li^+ can be efficiently transferred to TiO_2. As seen in the inset of Fig.5 Y_2SiO_5: 7.2% Pr^{3+}, 9% Li^+ can be efficiently excited by blue green-light (460nm-520nm) in visible-light region. So, Y_2SiO_5: Pr^{3+}, Li^+/TiO_2 composites can be efficiently excited by photons with light wavelengths longer than about 400 nm in the visible-light range, which enables more efficient use of solar energy.

3.3 Photocatalytic activity and mechanism

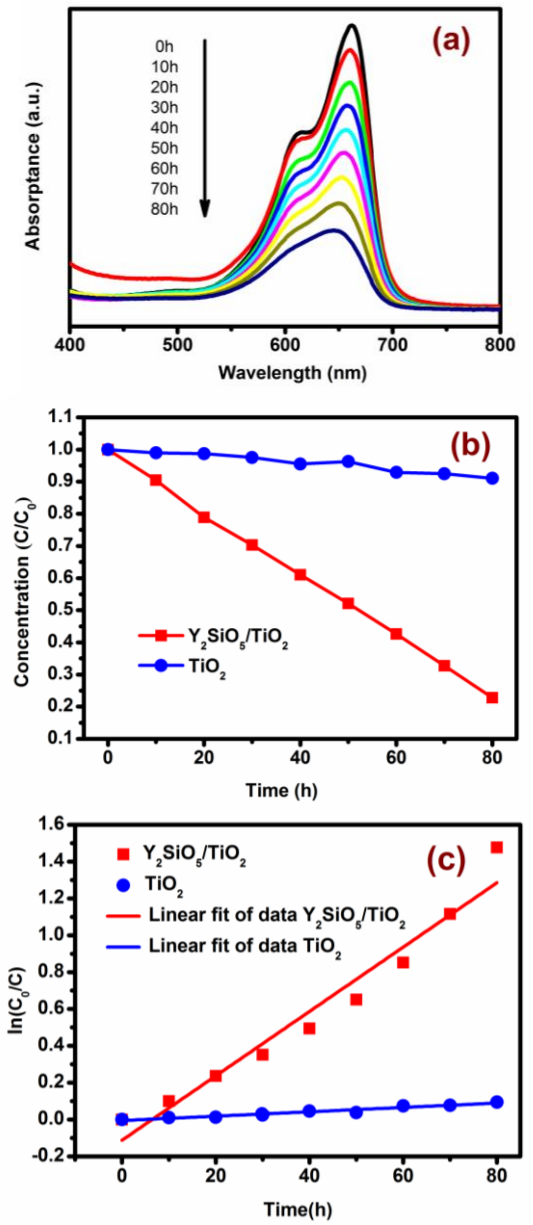

Fig.6 (a) Variation in absorbance spectra of MB photocatalyzed by Y_2SiO_5: Pr^{3+}, Li^+/TiO_2 as a function of the irradiation time under a 500 W xenon lamp irradiation. (b) comparison of the normalized concentration of MB decomposed by Y_2SiO_5: Pr^{3+}, Li^+/TiO_2 and TiO_2. (c) the photodegradation reaction kinetics data of Y_2SiO_5: Pr^{3+}, Li^+/TiO_2 composites and TiO_2.

From the previous section, it can be seen that Y_2SiO_5: Pr^{3+}, Li^+ can be efficiently excited by a xenon lamp 150W and UV upconversion emisson can be efficiently transferred to TiO_2. In this section, the decolorization of MB was carried out to verify the photocatalytic activity of Y_2SiO_5: Pr^{3+}, Li^+/TiO_2 catalysts under visible-light by the 500W xenon lamp. Fig.6 (a) showed the absorption spectra of MB catalyzed by the Y_2SiO_5: Pr^{3+}, Li^+/TiO_2 composites as a function of irradiation time. With the increase of irradiation time, the strong absorption band at 664 nm decreased steadily. This result clearly demonstrated that the obtained composites could be used to decompose MB by visible light, as predicted. The changes in concentration of C/C_0 with different exposure times were plotted in Fig.6 (b), where C_0 was the original concentration of MB and C was the concentration of MB irradiated with a 500 W xenon lamp for time t. The degradation efficiency could be evaluated through the change of the MB concentrations before and after irradiation. Fig.6 (b) indicated that 80% of MB was decomposed after 80 h irradiation by Y_2SiO_5: Pr^{3+}, Li^+/TiO_2 composites, which was far higher than that by pureTiO_2. First-order fitting of the $\ln(C/C_0)$ versus time for the photodegradation was usually used to study the reaction kinetics. Based on the photodegradation rate of MB with time, the photodegradation reaction kinetics lines were drawn out, as shown in Fig.6(c). According to the reaction kinetics linear equation and correlation indexes: $-\ln(C/C_0) = 0.01747t-0.11227$, R = 0.97520, $-\ln(C/C_0) = 0.00119t-0.00555$, R = 0.96991, for Y_2SiO_5: Pr^{3+}, Li^+/TiO_2 composites and pure TiO_2, respectively, it clearly presented that the rate constant for Y_2SiO_5: Pr^{3+}, Li^+/TiO_2 composites (0.01747) was about 14 times as high as that for pure TiO_2 (0.00119). All of these results implied that the degradation reaction of MB in the visible light follows the first-order kinetic law.

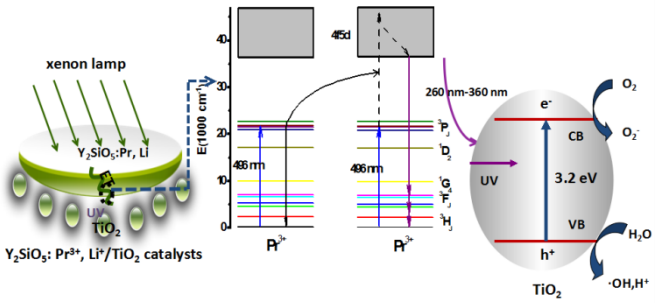

Fig.7 Photocatalysis mechanism of Y_2SiO_5: Pr^{3+}, Li^+/TiO_2 catalyst (ET: energy transfer).

To explain the above phenomenon, the photocatalysis mechanism of Y_2SiO_5: Pr^{3+}, Li^+/TiO_2 catalyst was discussed. In Y_2SiO_5: Pr^{3+}, Li^+/TiO_2 composite, Pr^{3+} ion only exists in Y_2SiO_5 host. Fig.7 showed the energy transfer upconversion (ETU) mechanism between neighboring Pr^{3+} ions and TiO_2. The population of ^3P_J states via blue photon absorption and the subsequent energy transfer between ions could promote an electron to the 4f5d energy band, resulting in the emission of UVB- and UVC-range photons which corresponding to 4f5d $\rightarrow {}^3H_J/{}^3F_J$.[45, 46] Then TiO_2 was excited by the ultraviolet-light photon. The activated TiO_2 produced reductive electrons (e^-) and oxidative holes (h^+) in the conduction band (CB) and the valence band (VB), respectively, and these electron–hole pairs migrated from the inner region to the surfaces to take part in surface reactions. Eventually, hydroxyl radical (· OH), O_2^{2-} and H^+ were formed.[47] The product can mineralize the organic chemicals and it could also destroy the chromophore position. Obviously, from the above photocatalysis mechanism, the photocatalytic activity of Y_2SiO_5: Pr^{3+}, Li^+/TiO_2 composite depended strongly on the contact area between Y_2SiO_5: Pr^{3+}, Li^+ and TiO_2 particles. To enhance the TiO_2 photocatalysis behavior, it is necessary to enlarge the contact area between Y_2SiO_5: Pr^{3+}, Li^+ and TiO_2 particles.

4. Conclusions

The upconversion luminescence agents that can be effectively excited by the ordinary illumination sources (fluorescent lamp or xenon lamp) have broad applying prospect in biology, medicine, environment and soon. In this paper, Pr^{3+} doped Y_2SiO_5 upconversion nanomaterials can be effectively excited by the blue light from a xenon lamp 150W with grating as its light splitter. The obtained data indiated that UV upconversion emssion can be effectively transferred to TiO_2. All of these performances ensure the Y_2SiO_5: Pr^{3+}, Li^+/TiO_2 composites to be a good visible light catalyst.

Acknowledgements

This work was supported by National Science Foundation of China (No. 11474083), Hebei Province Department of Education Fund (ZD2014069).

Notes and references

The Midwest universities comprehensive strength promotion project, Hebei Key Lab of Optic-electronic Information and Materials, College of Physics Science and Technology, Hebei University, Baoding 071002, China
E-mail: mihuyym@163.com
**Corresponding author. Fax & Tel.: 86159 3028 4830*
‡ These authors contribute equally to this work.

1 S. Shen, J. Chen, X. Wang, L. Zhao and L. Guo, *Journal of Power Sources*, 2011, **196**, 10112-10119.
2 G. Kim, S.H. Lee, W. Choi, *Applied Catalysis B: Environmental*, 2015, **162**, 463-469.
3 D.X. Xu, Z.W. Lian, M.L. Fu, B. Yuan, J.W. Shi, H.J. Cui, *Applied Catalysis B: Environmental*, 2013, **142-143**, 377-386.
4 Z. Zhang and W. Wang, *Dalton transactions*, 2013, **42**, 12072-12074.
5 Y. He, Y. Wang, L. Zhang, B. Teng and M. Fan, *Applied Catalysis B: Environmental*, 2015, **168-169**, 1-8.
6 Z. Gao, Z. Cui, S. Zhu, Y. Liang, Z. Li and X. Yang, *Journal of Power Sources*, 2015, **283**, 397-407.
7 K. Nakata and A. Fujishima, *Journal of Photochemistry and Photobiology C: Photochemistry Reviews*, 2012, **13**, 169-189.
8 A. Fujishima and X. Zhang, *Comptes Rendus Chimie*, 2006, **9**, 750-760.
9 Y. Chen, S. Mishra, G. Ledoux, E. Jeanneau, M. Daniel, J. Zhang and S. Daniele, *Chemistry, an Asian journal*, 2014, **9**, 2415-2421.
10 Q. Yin, R. Qiao, L. Zhu, Z. Li, M. Li and W. Wu, *Materials Letters*, 2014, **135**, 135-138.
11 L.W. Zhang, H.B. Fu and Y.F. Zhu, *Advanced Functional Materials*, 2008, **18**, 2180-2189.
12 Y.H. Ng, S. Ikeda, M. Matsumura and R. Amal, *Energy & Environmental Science*, 2012, **5**, 9307-9318.
13 J. Reszczyńska, T. Grzyb, J. W. Sobczak, W. Lisowski, M. Gazda, B. Ohtani and A. Zaleska, *Applied Catalysis B: Environmental*, 2015, **163**, 40-49.
14 D. Hou, R. Goei, X. Wang, P. Wang and T.T. Lim, *Applied Catalysis B: Environmental*, 2012, **126**, 121-133.
15 A. Zaleska, P. Górska, J. W. Sobczak and J. Hupka, *Applied Catalysis B: Environmental*, 2007, **76**, 1-8.
16 X. Guo, C. Chen, W. Song, X. Wang, W. Di and W. Qin, *Journal of Molecular Catalysis A: Chemical*, 2014, **387**, 1-6.
17 S. Guo, D. Li, Y. Zhang, Y. Zhang and X. Zhou, *Electrochimica Acta*, 2014, **121**, 352-360.
18 C. Li, F. Wang, J. Zhu and J. C. Yu, *Applied Catalysis B: Environmental*, 2010, **100**, 433-439.
19 H. Wang, G. Wang, Y. Ling, M. Lepert, C. Wang, J. Z. Zhang and Y. Li, *Nanoscale*, 2012, **4**, 1463-1466.
20 Y. Zhu, Z. Chen, T. Gao, Q. Huang, F. Niu, L. Qin, P. Tang, Y. Huang, Z. Sha and Y. Wang, *Applied Catalysis B: Environmental*, 2015, **163**, 16-22.
21 Y. Li, K. Pan, G. Wang, B. Jiang, C. Tian, W. Zhou, Y. Qu, S. Liu, L. Feng and H. Fu, *Dalton transactions*, 2013, **42**, 7971-7979.
22 X. Guo, W. Song, C. Chen, W. Di and W. Qin, *Physical chemistry chemical physics : PCCP*, 2013, **15**, 14681-14688.
23 J. Méndez-Ramos, P. Acosta-Mora, J. C. Ruiz-Morales, T. Hernández, M. E. Borges and P. Esparza, *RSC Advances*, 2013, **3**, 23028.
24 Y. Yang, C. Mi, F. Jiao, X. Su, X. Li, L. Liu, J. Zhang, F. Yu, Y. Liu, Y. Mai and J. Ballato, *Journal of the American Ceramic Society*, 2014, **97**, 1769-1775.
25 Y. Yang, C. Mi, F. Yu, X. Su, C. Guo, G. Li, J. Zhang, L. Liu, Y. Liu and X. Li, *Ceramics International*, 2014, **40**, 9875-9880.
26 S. Huang, Z. Lou, Z. Qi, N. Zhu and H. Yuan, *Applied Catalysis B: Environmental*, 2015, **168-169**, 313-321.
27 X. Guo, W. Di, C. Chen, C. Liu, X. Wang and W. Qin, *Dalton transactions*, 2014, **43**, 1048-1054.
28 W. Qin, D. Zhang, D. Zhao, L. Wang and K. Zheng, *Chemical communications*, 2010, **46**, 2304-2306.
29 Y. Tang, W. Di, X. Zhai, R. Yang and W. Qin, *ACS Catalysis*, 2013, **3**, 405-412.
30 F. Qin, Y. Zheng, Y. Yu, C. Zheng, H. Liang, Z. Zhang and L. Xu, *Journal of Luminescence*, 2009, **129**, 1137-1139.
31 H. Guo, Y. Li, D. Wang, W. Zhang, M. Yin, L. Lou and S. Xia, *Journal of Alloys and Compounds*, 2004, **376**, 23-27.
32 J. Wang, R. Li, Z. Zhang, W. Sun, R. Xu, Y. Xie, Z. Xing and X. Zhang, *Applied Catalysis A: General*, 2008, **334**, 227-233.
33 S. Obregon and G. Colon, *Chemical communications*, 2012, **48**, 7865-7867.
34 L. Yin, Y. Li, J. Wang, Y. Zhai, J. Wang, Y. Kong, B. Wang and X. Zhang, *Environmental Progress & Sustainable Energy*, 2013, **32**, 697-704.
35 S. L. Guangjian Feng, Zhiliang Xiu,Yin Zhang,Jiaoxian Yu,Yonggang Chen,Ping Wang,and Xiaojun Yu, *J. Phys. Chem. C*, 2008, **112**, 13692–13699.
36 S. Li, Y. Guo, L. Zhang, J. Wang, Y. Li, Y. Li and B. Wang, *Journal of Power Sources*, 2014, **252**, 21-27.
37 Y. Yang, C. Zhang, Y. Xu, H. Wang, X. Li and C. Wang, *Materials Letters*, 2010, **64**, 147-150.
38 Y. Zheng and W. Wang, *Journal of Solid State Chemistry*, 2014, **210**, 206-212.
39 S. Obregón, A. Kubacka, M. Fernández-García and G. Colón, *Journal of Catalysis*, 2013, **299**, 298-306.
40 Y. Yang, C. Mi, X. Su, F. Jiao, L. Liu, J. Zhang, F. Yu, X. Li, Y. Liu and Y. Mai, *Optics Letters*, 2014, **39**, 2000.
41 E. L. Cates and J.-H. Kim, *Optical Materials*, 2013, **35**, 2347-2351.
42 E. L. Cates, M. Cho and J. H. Kim, *Environmental science & technology*, 2011, **45**, 3680-3686.
43 B. Mitu, S. Vizireanu, R. Birjega, M. Dinescu, S. Somacescu, P. Osiceanu, V. Pârvulescu and G. Dinescu, *Thin Solid Films*, 2007, **515**, 6484-6488.
44 E. L. Cates, A. P. Wilkinson and J.-H. Kim, *The Journal of Physical*

Chemistry C, 2012, **116**, 12772-12778.
45 S. L. Cates, E. L. Cates, M. Cho and J. H. Kim, *Environmental science & technology*, 2014, **48**, 2290-2297.
46 C. L. Sun, J. F. Li, C. H. Hu, H. M. Jiang and Z. K. Jiang, *The European Physical Journal D*, 2006, **39**, 303-306.
47 Q. Kang, Q. Z. Lu, S. H. Liu, L. X. Yang, L. F. Wen, S. L. Luo and Q. Y. Cai, *Biomaterials*, 2010, **31**, 3317-3326.